Interferometry

Xin Gao

1 Abstract

Using 1-D, 2-array interferometry, we calculate the baseline length of our inferometer and the size of the source objects in the sky. Our sources are the Sun, the Moon, and a point source, the Orion Nebula. In our analysis of the Orion Nebula, we use a least-squares fitting method to calculate the baseline length of the interferometer to be 9.925, slightly off from the approximate but used value of 10. We then similarly used it along with fringe response equations to derive the size of the Sun and the Moon in the sky. Their resulting angular values are close to one another as expected; otherwise, there would be no total solar eclipses.

2 Introduction

Interferometry is a core method in radio astronomy for collecting and analyzing data. An interferometer consists of at least two dish telescopes that capture signals in radio frequencies. The distance of separation, or the baseline, is crucial in its design; the precise length determines the phase difference, if any, of a source signal, which can be used to extract the declination of the source. It determines the time difference, or geometric delay, between the reception of the signal by the telescopes. This delay is used with multiple signals in the method of correlation to image the sources. The baseline determines also the phase difference with a corresponding wavelength or frequency. This difference can graphically respresent the signals, manifesting as sinusoidal 'fringe patterns.' Our analyses use these fringe patterns, along with statistical and mathematical tools, to derive characteristics of sources such as their celestial declination, their corresponding brightness distributions, and, in the case of nearby physically distinguishable objects such as the Sun and the Moon, their diameter.

3 Background: Astrophysics and Conventions for Interferometry

When studying space, astronomers have to determine a point of reference for assigning coordinates to objects. There are several conventional coordinate systems, based on difference reference frames. Similarly, time conventions exist for determining locations of objects at a particular time. How astronomers measure light data is also important for having defined conventions for consistency and communication.

3.1 Time Conventions for Astronomers

From the definition of the day to the beginning of dates, astronomers tend to mess with time for practical purposes.

3.1.1 The Legacy of Julius

The dominant dating system being used today is the Gregorian calendar. In astronomy, Julian dates are used instead. The Julian date began at noon of present-day England on January 1st, 4713 B.C. and is counted in solar days. This convention serves as an universal dating method for astronomers, eliminating confusion due to using different systems. The Julian Date operates in 7980 year cycles, a value carefully chosen for convenience and for converting among other dating systems.

3.1.2 Solar Days vs. Sidereal Days

We use the solar day system for our daily lives; that is, we judge the time of the day by the location of the sun in the sky. Because that Earth slightly moves its location relative to the sun every day, a solar day exceeds 2π radians about the rotation of the Earth on it axis. A sidereal day describes the amount of time that it takes Earth to rotate exactly 360 degrees, which results in it lasting approximately 23 hours and 56 minutes. This convention in the form of Local Sidereal Time (LST) is useful for calculating the hour angle; this will be explored further.

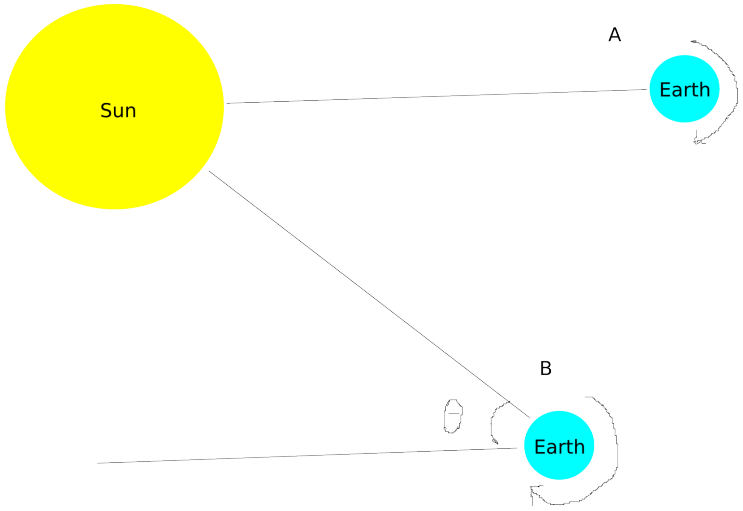

Figure 1: Solar Day vs. Sidereal Day. From point A to point B, the Earth made an angle θ relative to its orbit around the Sun. The difference in time of day -for example, the meaning of 'noon'- is also described by θ relative to Earth's rotation about its axis.

3.2 Celestial Reference Frames: Coordinate Systems

How should we describe the location of an object in the sky? There are many answers with several conventions to choose from. For our purposes, the topocentric, hour angle, and equatorial coordinates are of interest. If one sees a star directly overhead, you might be inclined to assign that star an altitude of 90 degrees (zenith). This is in the reference frame of an individual and the coordinates of an object are known as to be in topocentric coordinates, measuring an object's azimuth and altitude **(az, alt)**. Azimuth value begins at the north direction and goes counterclockwise. This is convenient for an individual, but lacks meaning for global communication. For distant objects, they are in a somewhat fixed position in the sky over long periods of human time. The equatorial coordinate system, in the reference frame of the Earth, assigns a fixed coordinate to each celestial object with a right ascension and declination value $\mathbf{(r\alpha, \delta)}$ based on its position on the celestial sphere. An object in the direction of the sun at vernal equinox has a right ascension value, measured in hours from 0 to 24, of 0. Increasing values of right ascenion goes with the the path of the sun along the elliptic. An object along the celestial equator has a declination of 0 degrees. The LST

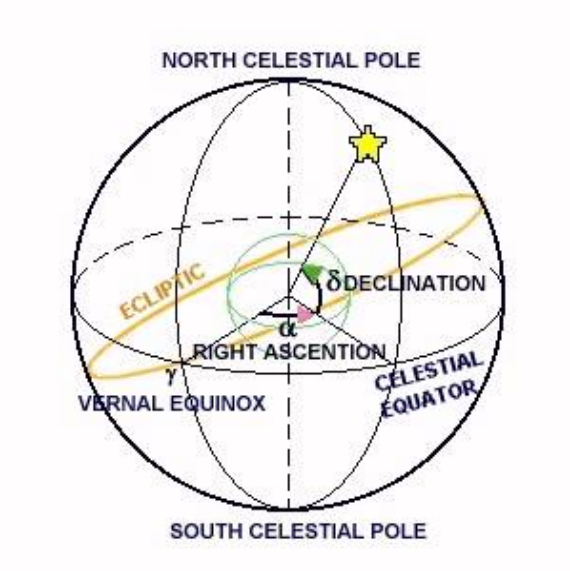

Figure 2: Geocentric Equatorial Coordinates with the solar direction on spring equinox at the equator, γ, being the origin.

is the current time at a location based on sidereal days. The hour angle of an object is its right ascension subtracted by the LST. The hour angle coordinate **(ha, δ)** describes the right ascension of an object based on an individual's reference frame but maintains the fixed declination value. We often use equatorial coordinates and topocentric coordinates with hour angles coordinates serving as an intermediate system. One set of coordinate values can be mathematically transformed to that

of another by rotation matrices. The matrix to go from equatorial to hour angle is:

$$R_{r\alpha,\delta\to ha,\delta} = \begin{bmatrix} cos(LST) & sin(LST) & 0 \\ sin(LST) & -cos(LST) & 0 \\ 0 & 0 & 1 \end{bmatrix} \tag{1}$$

and the matrix to go from hour angle to topocentric is:

$$R_{ha,\delta\to az,alt} = \begin{bmatrix} -sin(\phi) & 0 & cos(\phi) \\ 0 & -1 & 0 \\ cos(\phi) & 0 & sin(\phi) \end{bmatrix} \tag{2}$$

where ϕ is latitude of a location in degrees. To go straight from equatorial to topocentric coordinates, multiply these two matrices of transformation together in the opposite order. The inverse of this resulting matrix can be used to go back to equatorial from topocentric coordinates. We make a python program (in the file rotation_matrix.py) to convert coordinates when necessary. Using the sys module, we input topocentric coordinates for equatorial coordinates as output.

3.2.1 Perception of Light; Units of Radiation

There are many ways to categorize data and how we interpret it. Power is an enticing but inconsistent way to measure it since it's dependent on telescope size. Other factors, such as difference distance to source range of measurable light frequencies result in variance from different measurements. Flux ignores telescope size by taking into account per area, but is also variant, depending on the distance to the source; a location farther away from the source measures a lower flux since the source will appear smaller and thus its light more spread apart. Surface brightness corrects the distance differences by taking into account per steradian, a unit of solid angle, which is the apparent size of the source as determined by how much of the sky it takes up. Flux density instead corrects the variance due to the measurable radiation range of different telescopes by including per frequency. Specific intensity I is the invariant method of measuring light; it takes into account the area of the receiver, the apparent size of the source, and a specific frequency:

$$I(P, A, \Omega, \nu) = \frac{P}{A \times \Omega \times \nu} \tag{3}$$

where P is power, A is area of receiver, Ω is solid angle, and ν is frequency. The unit of spectral intensity is often expressed in jansky (Jy) per steradian where the jansky is defined as:

$$1Jy \equiv 10^{-26} \frac{W}{m^2 \cdot Hz} \tag{4}$$

The invariance of specific intensity allows for consistent analysis.

4 Methods and Procedure

We begin with exploring the design of an interferometer and the physics behind the data analysis. Once we have collected the data, we extract characteristics of the sources using our program and physical and statistical methods, such as least-squares fitting.

4.1 From Signal to Image

Let's look at the simple example of a two-telescope interferometer separated by the baseline $\overrightarrow{\mathbf{b}}$. A source in the direction of $\hat{\mathbf{s}}$ is emitting signals which are received by the telescopes at different times. The extra distance travels by the signal to the second telescope is thus $\overrightarrow{\mathbf{b}} \cdot \hat{\mathbf{s}} = bcos\theta$. Since the signal is electromagnetic radiation, we divide the extra distance by c to obtain the geometric time delay τ:

$$\tau = \frac{\overrightarrow{\mathbf{b}} \cdot \hat{\mathbf{s}}}{c} \tag{5}$$

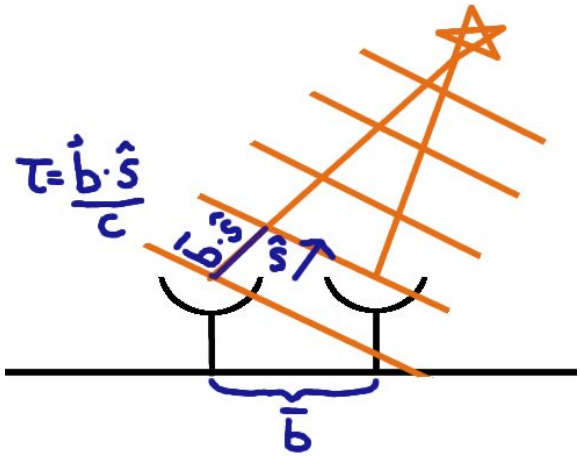

Figure 3: Two-interferometer system showing the derivation of the geometric delay. Meticulous art by Aaron Parsons, PhD.

4.1.1 Correlation Theorem and the Architecture of Data Synthesis

Correlation is a mathematical tool for determining the 'similarity' level of data, or in a specific case, how alike are different signals over a time period. The correlation of two functions is the integral of the fourier transform of one function times the conjugated fourier transform of the other function:

$$(f \star g)(\tau) = \int \hat{f}(\omega)\hat{g}^*(\omega)e^{i\omega t}d\omega \tag{6}$$

For interferometry, we take g(t) to be f(t-τ), where τ is the geometric delay, to correlate data received by one radio telescope with a delayed but similar signal received by another telescope. The correlation relation can thus be written as:

$$f(t) \star f(t-\tau) = \int \hat{f}(\omega)\frac{1}{2\pi}\hat{f}^*(\omega)e^{i\omega t-\tau}d\omega \tag{7}$$

$$= \left|f^2\right| \int \frac{1}{2\pi} e^{i\omega t - \tau} d\omega = \left|f^2\right| \cdot \delta(t - \tau) \tag{8}$$

It turns out that when two similar signals separated by a time delay get correlated, the result is a delta function. The measurement as power as function of time has peaks at the delay (positive and negative τ); correlation can be used to determine and geometric delay and thus, as we shall see, the precise length of the baseline. In radio astronomy, data is often preferred in frequency domain and is the case for the output of a correlator. This process becomes cumbersome when dealing with large amounts of data from a large array of telescopes, but programs are designed to lighten the load. There are two types of correlators: FX and XF architectures. in the XF design, the signals are correlated first and then fourier transformed. This can take heavy amounts of processing because, for an array of N telescopes, there are $\frac{N}{2}(N+1)$ correlations and thus such number of fourier transformations to computer. In the more common and efficient FX architecture, the fourier transforms are computer first, so that there are only N computations, and then the correlations take place. FPGAs are the primary tools for the computations with GPUs occasionally assist in the correlation.

4.1.2 There's a Correlation! Duo-Signal Interferometry

We now have two sets of data each with its own geometric delay τ_1 or τ_2. We correlate the corresponding signals as functions f and g with $f(t) = f_1(t) + f_2(t)$ and $g = f(t-\tau) = f_1(t-\tau_1) + f_2(t-\tau_2)$:

$$f \star g(\tau) = \int f(t) f^*(t-\tau) dt \tag{9}$$

$$= \int f_1(t) f_1(t - \tau_1 - \tau) f_2(t) f_2(t - \tau_2 - \tau) dt \tag{10}$$

$$= \int f_1(t) f_1(t) dt =< e_1^2 > \tag{11}$$

Equation 7 is the correlation equation. Equation 8 is obtained by multiplying out the terms in the integrand and eliminating the product terms of $f_1(t) and f_2(t)$, which are integrated to 0. We then set $\tau = -\tau_1$ or $-\tau_2$ to get either a factor of f_1^2 or f_2^2 with the other one integrated to 0. The result in equation 9 is an amplitude at $-\tau_1$ or $-\tau_2$, as expected from the delta function result from the correlation theorem. There will be noise generated from other sources from the sky. Two telescopes can provide only 1-D images since the geometric delay accounts for only 1 direction; larger arrays can provide 2-D images, reflecting what is seen in the sky.

4.1.3 Dirtying the Sky; The Visibility Equation

It's useful to first limit ourselves to a single frequency ν since our analyses are often frequency dependent. We write the geometry delay in terms of ν:

$$\tau\nu = \frac{\overrightarrow{\mathbf{b}} \cdot \hat{\mathbf{s}}}{\lambda} \tag{12}$$

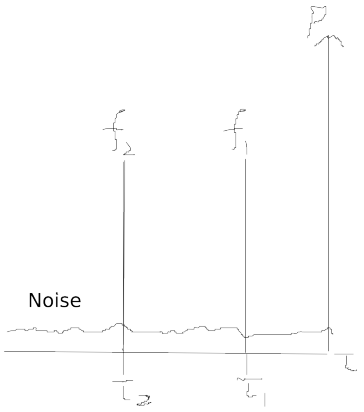

Figure 4: Graphical representation of the correlated data with peaks at the corresponding delays

This delay gives rise to a phase difference denoted by:

$$\Delta\phi = e^{-i\theta} = e^{2\pi i \frac{\vec{\mathbf{b}}\cdot\hat{\mathbf{s}}}{\lambda}} \tag{13}$$

This complex factor in term produces a somewhat sinusoidal fringe pattern while the real component produces a image of the sky with the source, both as a function of distance along the sky. With this information, it is possible to map the sky with one baseline, representing what a larger array can image. We split the baseline into its three components of east-west, north-south, and depth $\frac{\vec{\mathbf{b}}}{\lambda} = (u, v, w)$. Similarly, we separate the directional unit vector $\hat{\mathbf{s}}$ into east-west, north-south, and unit factor components $(l, m, \sqrt{1-l^2-m^2}$. By integrating the intensity I(l,m) with the response of the primary antenna beams A(l,m) and the phase shift, we get the visibility, or measurement, of the sky:

$$V(u,v) = \int\int A(l,m)\cdot I(l,m)\cdot e^{-2\pi i \frac{\vec{\mathbf{b}}\cdot\hat{\mathbf{s}}}{\lambda}} dldm \tag{14}$$

$$= \int\int A(l,m)\cdot I(l,m)\cdot e^{-2\pi i(ul+vm+w\sqrt{1-l^2-m^2})} \tag{15}$$

$$\approx e^{-2\pi iw}\int\int A(l,m)\cdot I(l,m)\cdot e^{-2\pi i(ul+vm)} \tag{16}$$

Assuming l and m to be much smaller than 1, a valid assumption, the integral simplifies down to Equation 14. The visibility equation is the fourier transformation of the sky from spatial (angular) domain to wavelength (inverse angular) domain, whose corresponding image is the $'u - vplane'$. Data from a pair of telescopes come in two samples: values for positive and negative u and v; that is, there are measurements of V and V^*. Taking different values for baseline and computing the visibility produces the sampling pattern of the sky and its corresponding $'real'$ image of the sky known as the $'dirtybeam'$. The sampling pattern samples the true u-v plane, resulting in a $'dirty'$ image of the sky, where the dirtying refers to a messy image due to information loss from the sampling. The image can be cleaned by deconvolution, a method that involves providing

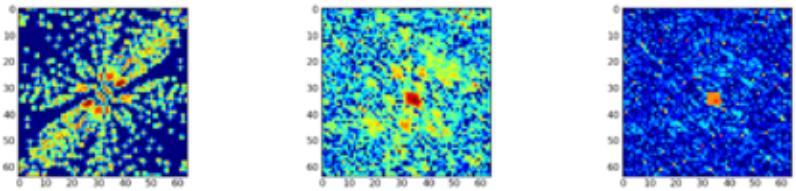

Figure 5: Example of the visibility imaging process, courtesy of radio astronomer Aaron Parsons, PhD. Left: the sampling pattern; middle: the dirtied image; right: the cleaned image

prior-known information of the real sky to improve the smoothness of the resulting image.

4.1.4 Resolution and the Limits of Observation

Resolution is limited by the nature of light. The diffraction limit under perfect observing conditions is the observed angle about which an image can be resolved and the angle is related to light and your instrument by:

$$\theta \approx 1.22\frac{\lambda}{D} \tag{17}$$

λ is the wavelength of the signals received and D is the diameter of the telescope. Radio astronomical observations are minimally affected by confounding factors in the atmosphere at appropriate location so this diffraction limit holds true. The long wavelength of radio waves makes it somewhat difficult to resolve very distant sources, but this problem is alleviated by using an array of dishes with large values, B of the baseline that replace D.

4.2 Least-Squares Fitting and Determining the Baseline

The fringe data provides us with much information, including the precise baseline of our interferometer or the precise declination of our point source. Only one component of our baseline matters since we're working with a two-telescope array and we denote this baseline component by B_y. The delay of signal reception is actually more than just the geometric delay due to electronics in the

cable: $\tau_{total} = \tau_{geo}(h_s) + \tau_{cable}$ where h_s is the hour angle of the point source. τ_{geo} can be written as a function of B_y, declination δ, and h_s:

$$\tau_g(h_s) = \frac{B_y}{c} cos(\delta) sin(h_s) \tag{18}$$

From this, we get the total fringe voltage:

$$F(t) = E_1(t) \cdot E_2(t) = cos(2\pi\nu t) \cdot cos(2\pi\nu[t + \tau_{total}]) \tag{19}$$

Using trigonometric manipulating and changing the frequency ν dependence to wavelength λ dependence, we arrive at the Fringe Amplitude Equation that describes our data:

$$F(h_s) = Acos[2\pi(\frac{B_y}{\lambda} cos(\delta)) sin(h_s)] - Bsin[2\pi(\frac{B_y}{\lambda} cos(\delta)) sin(h_s)] \tag{20}$$

The coefficients are defined as A $\equiv cos(\frac{2c\pi\tau_{cable}}{\lambda})$ and B $\equiv cos(\frac{2c\pi\tau_{cable}}{\lambda})$. This equation is now ripe to be used with least-squares fitting on point source data. Least-squares fitting is a method of fitting a data set to a type of curve that best represents the data set. Our goal is to determine either the baseline or the declination, but not both because you have to assume one to solve for ther other as a variable. For convenience we define C $\equiv [2\pi(\frac{B_y}{\lambda} cos(\delta))]$, reducing the equation to:

$$F(h_s) = Acos[Csin(h_s)] - Bsin[Csin(h_s)] \tag{21}$$

The hour angle h_s can be obtained using your local sidereal time and the right ascension of the source. Our least-squares method ultimately outputs values of the residuals of our data. We plot the values of the residuals against C and the C value corresponding to the lowest residual value can be used to solve either δ or or B_y by assuming one.

4.3 The Size of Round Stuff in the Sky

A core goal of the interferometer is to project waves corresponding to received data onto constructed images of the sky to represent the information in the signals. Over time, the movement of objects across its projected fringe pattern produces a fringe response from our interferometer. For point sources, the fringe response F(h) is well described by the Equation 20. For objects large enough to be distinguishable in the sky and thus cannot be desribed by a singular value of hour angle, their hour angle is a function is related to intensity distribution over the sky. We use this information and the fact that intensity as a function of hour angle is related to the source radius to derive the size of the sources.

4.3.1 Mapping Round Stuff in the Sky: Brightness Distribution

The hour angle of a sizable non-point source and the intensity disribution of the source is given by:

$$h_s = \frac{\int I(h) h dh}{\int I(h) dh} \tag{22}$$

This equation describes the hour angle of the source center as the mean of its intensity. We write the intensity of a non-center point of the source as $I(\Delta h)$ where Δh is the difference of the hour

angle between the non-center point and the center point $h - h_s$. To find the response $R(h)$ of such an 'extended' source in the sky, we multiply Equation 20 by intensity as a function of hour angle difference and integrate the equation over small changes in hour angle $d\delta h$:

$$F(h_s) = A \int I(\Delta h) cos[2\pi(\frac{B_y}{\lambda} cos(\delta)) sin(h_s)] d\Delta h + B \int I(\Delta h) sin[2\pi(\frac{B_y}{\lambda} cos(\delta)) sin(h_s)] d\Delta h \tag{23}$$

To simplify numerically and conceptually, we define the local fringe frequency $f_f = \frac{C}{2/pi} cos(\delta)$ where $C \equiv \frac{B_y}{\lambda} cos(\delta)$. Since the Sun and Moon have declinations near 0 around at the time of our observations,, we can simplify the equation with the approximation $C \approx \frac{B_y}{\lambda}$. Using trigonometric identities and this definition, we come to:

$$R(h) = F(h) \cdot \int I(\Delta h) cos(2\pi f_f \Delta h) d\Delta h \tag{24}$$

Here, F(h) refers to the source center, corresponding to a Δ h value of 0. The integral part of the equation is the theoretical modulation function, the intensity distribution of the source across the sky in 1-D fourier space. The result of this equation, the brightness distribution, as fringe response as a function of anglular difference between source point and source center in the sky, appears symmetrically as an inverse parabola leveling off to constant value on either side. In fourier space, the result appears as a sinc function $\frac{sin(2\pi f_f R)}{2\pi f_f R}$ and the inverse domain can be in units of source diameter per fringe period. Analysis in this domain can lead to obtaining the radius of the source.

4.3.2 Discovering the Size: Theoretical Modulation

$I(\Delta h)$ is convenient for us because it can be function of the source radius, which is what we would like to know:

$$I(\Delta h) = \frac{\sqrt{(R^2 - \Delta h^2)}}{R} \tag{25}$$

where R is the radius of the point source. We then write the theoretical modulating function MF_{theory} in terms of R as well:

$$MF_{theory} = \frac{1}{R} \int \sqrt{(R^2 - \Delta h^2)} cos(2\pi f_f \Delta h) d\Delta h \tag{26}$$

We want to solve for source sizes numerically, so we divide the source intensity into 2N + 1 sections where the odd number chosen is for symmetry about the source center. Each division has a corresponding size and hour angle coverage of $\frac{R}{N} = \delta h$. The nth section thus spans an hour angle of $\Delta h_n = n\delta h$. The numerical form of the theoretical analytical modulating function is:

$$MF_{theorey} \approx \sum_{n=-N}^{+N} \sqrt{(R^2 - (n\delta h)^2)} cos(2\pi f_f n\delta h) \delta h \tag{27}$$

$$\approx \delta h \sum_{n=-N}^{+N} \sqrt{(1 - (\frac{n}{N})^2)} cos(\frac{2\pi f_f R n}{N}) \tag{28}$$

The summation equation is what is important to us. For large objects with a fringe phase offset, we first have to find the offset by using the least-squared method akin to what is done to determine the baseline. We then use the appropriate value for our numerical response equation. for The parameters at play here is are the fringe amplitude, source radius, and the local fringe frequency. There are certain values of R and f_f, related by $\frac{1}{f_s} = \frac{n}{2R}$, that correspond to 0 value for the amplitude. Once we have the these values of f_s, we can solve for the radius of our sources, the Sun and the Moon.

5 Data

Data is collected for three sources: the Sun, the Moon, and a distant point source, the Orion Nebula in our case. We track each source with the two-telescope interferometer approximately from its time of rise to its time of setting. We instruct the telescopes to track by providing to them our latitude ($+37.8732°$) and longitude ($-122.2573°$). The location to begin the observation is determined by the location of the source that that moment, which can be determined by its topocentric coordinates. For every observation, the direction of the telescope returns home every hour before continuing the data collection to prevent runaway tracking; there is a small gap once every 3600 seconds as shown in the plots. The initial data plots had their data points subtract out an average over a range to appear more clean and symmetric about the x-axis. It's sometimes useful to fourier filter the data to remove the outlier from having a significant amount of influence in analyses, but for our purposes the difference is negligible.

5.1 Solar Power

Data for the Sun, obtained over a span of about ten hours.

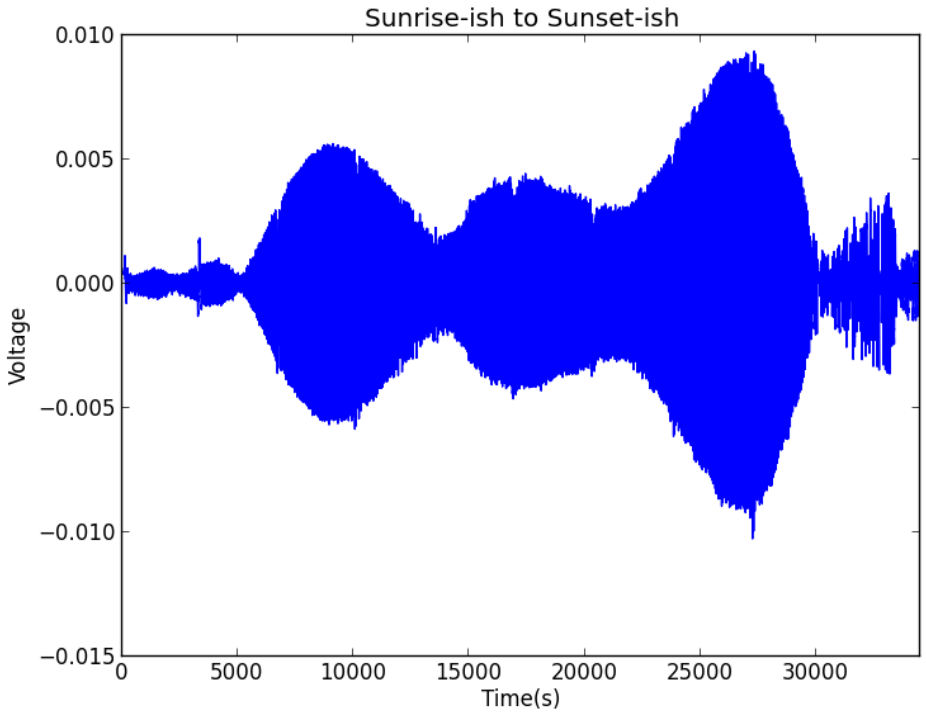

Figure 6: The fringe pattern of the sun from about sunrise to sunset

The Sun's data shape arises from its unique characteristics relative to us. Its rather large occupancy of solid angles in the sky and its sunspots influence the data we receive from it.

5.2 Lunar Radiance

Data for the Moon, obtained over nearly half a day.

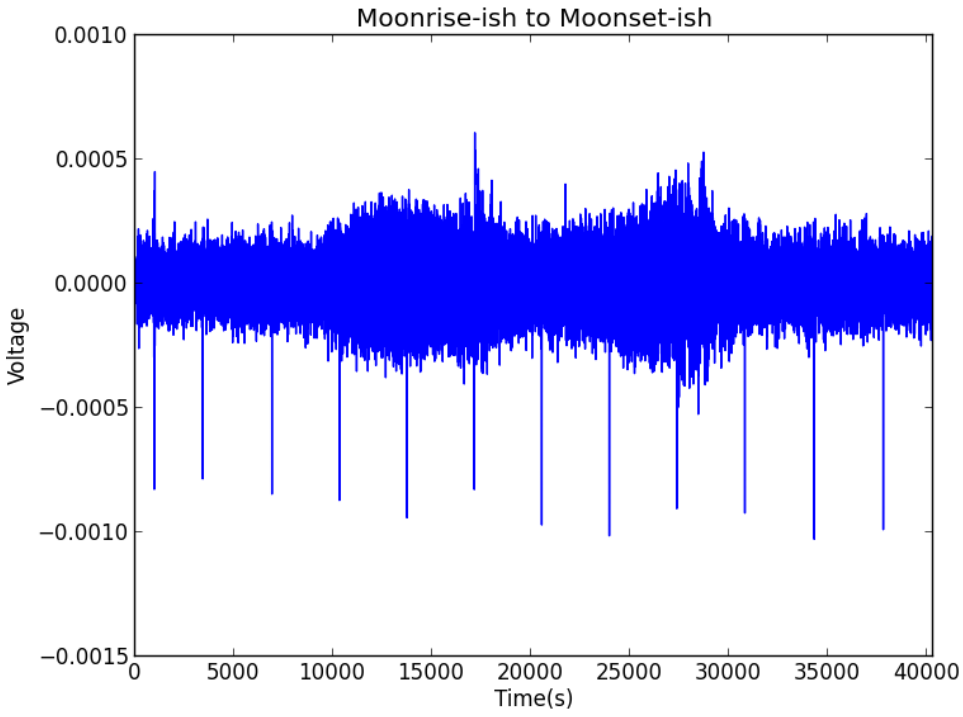

Figure 7: The fringe pattern of the moon from about moonrise to moonset

The Moon has a somewhat similar pattern to the Sun's but to less extremes. It is also very big in the sky.

5.3 Nebular Message

Data for the Orion Nebula:

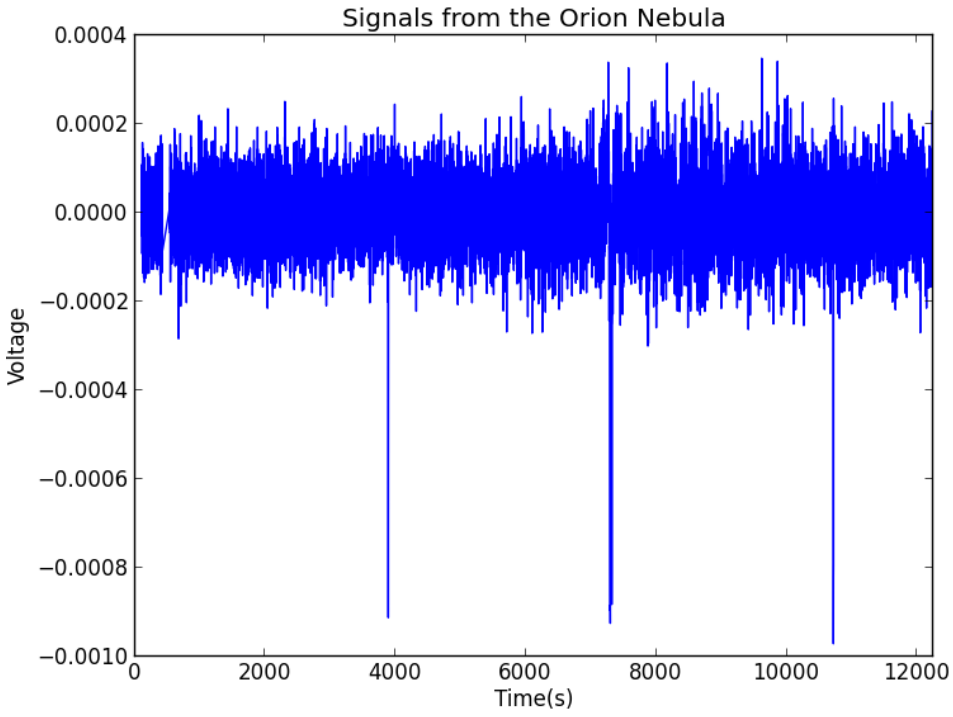

Figure 8: The fringe pattern of the nebula obtained over several hours

This graph is typical of that of a point source. It behaves more like a normal sinusoid than the Sun and Moon data.

6 Analysis and Discussion

We apply the methods described previously to our data. We use least-squares fitting and the mathematical equations to derive real-time characteristics of the Sun, Moon, and Orion Nebula from their data.

6.1 Interferometer Baseline Length Extraction from Orion Data

Recalling that C $\equiv [2\pi(\frac{B_y}{\lambda}cos(\delta))]$ with $\lambda = .028$ meter from the center frequency (10.67 GHz) our instrument operates on, we take δ to be the measured declination of the Orion Nebula in year 2000 (negligible difference to its present day value) to guess the correct value of for the baseline length of our interferometer. We know also that the baseline length is approximately 10 so we take values from 9.5 to 10.5 at increments of .001 as our guesses. We use the corresponding C values in our least-squares program to find an accurate value of the baseline, which is determined by the value

of C that returns the smallest value of the residual of our data. The following is the graphical representation of the resulting residual against C values.

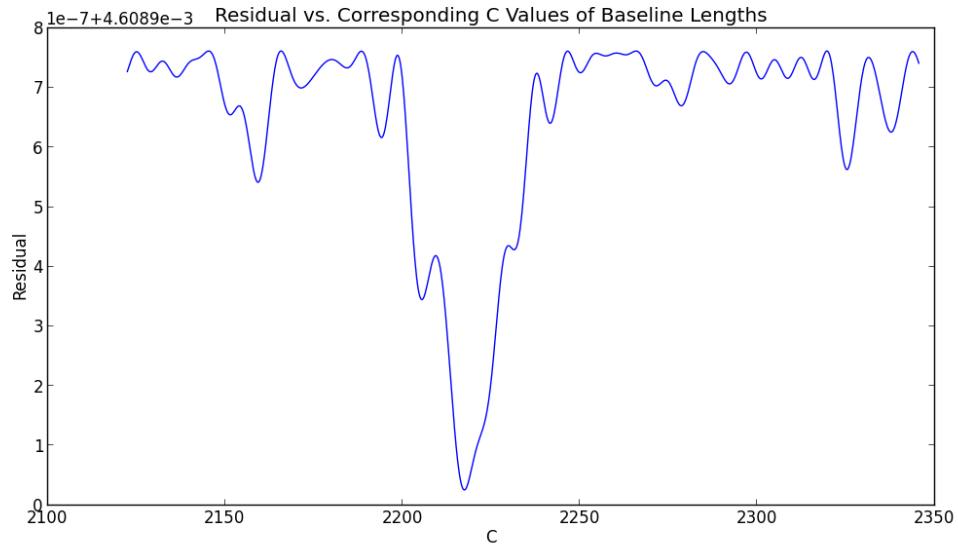

Figure 9: A plot of the residuals of the amplitudes of our Orion Nebula data against guessed values of C

The value of C corresponding to the smallest value of Residual is 2217.3145. Still assuming the aforementioned value for the declination, we arrive at the precise baseline value of **9.925 meters** for our interferometer. Again, it's also meaningful to apply this process to determine the declination of an object; we often can design our interferometer knowing its precise baseline length, which knowledge is used to pinpoint the location of objects in the sky and to determine the limits of our resolution.

6.2 The Waistlines of Sol and Luna

We find the radius of the Sun and the Moon using the fringe response equation. We are concerned with reproducing a real image so we use the cosine component:

$$F(h) = cos(C \cdot sin(h_S) \cdot \phi \tag{29}$$

Here C is defined as usual and ϕ is the phase offset of our fringe source. As aforementioned, for solar and lunar analyses, we assume $cos(\delta)$ so be approximately 1 due to the proximity of the sources' declinations to the celestial equator at the time of observation (near spring equinox). C reduces to $\approx 2\pi\frac{B_y}{\lambda}$. We use the baseline length we found: C $\approx$ 2494. Using the least-squares method, we find the value of ϕ for the Sun and the Moon.

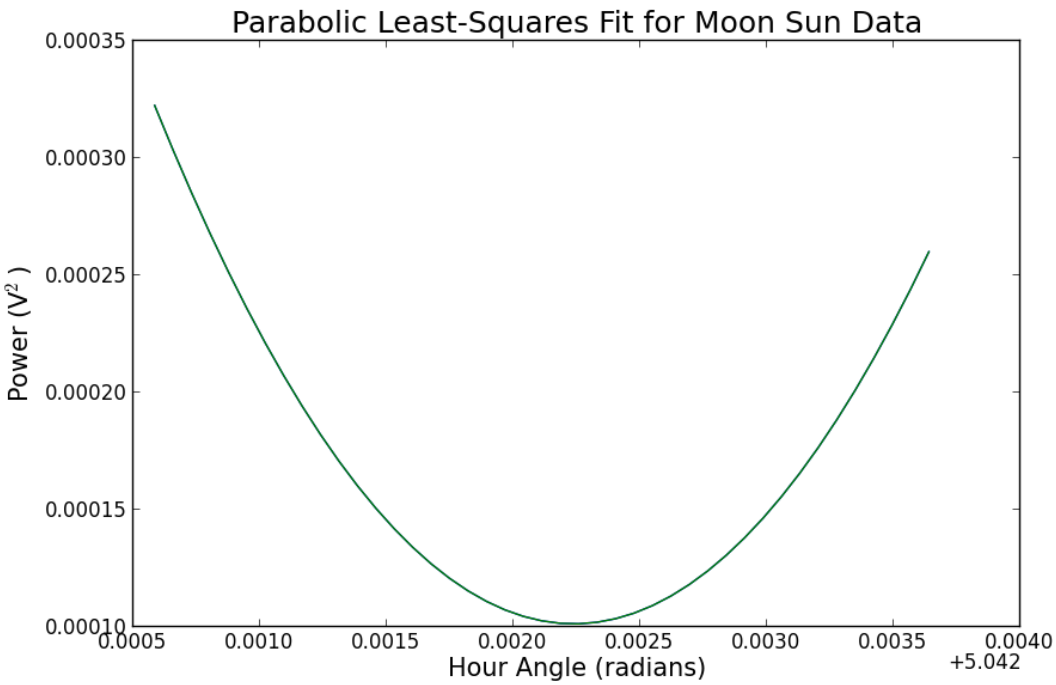

Figure 10: Least-squares fit for determining ϕ for the sun
The lowest value of the power corresponds to $\phi = 5.04428$ radians for the Sun.

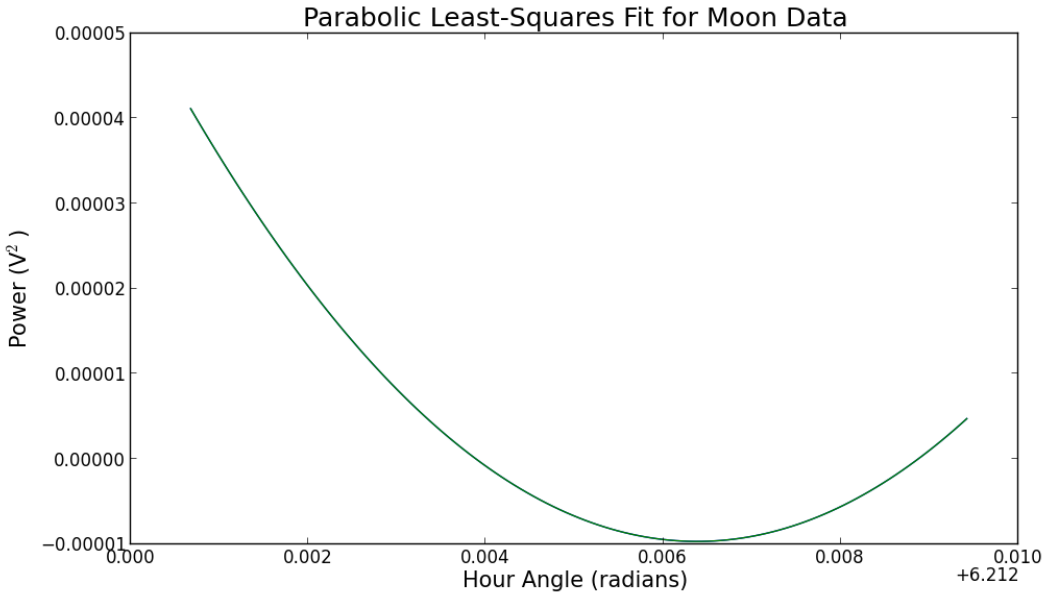

Figure 11: Least-squares fit for determining ϕ for the moon

The lowest value of the power corresponds to $\phi = 6.21836$ radians for the Moon. We use these ϕ values to solve for in our program the Bessel polynomial function corresponding to our numerical theoretical modulating function. We plot the resulting modulating function as a function of Rf_f.

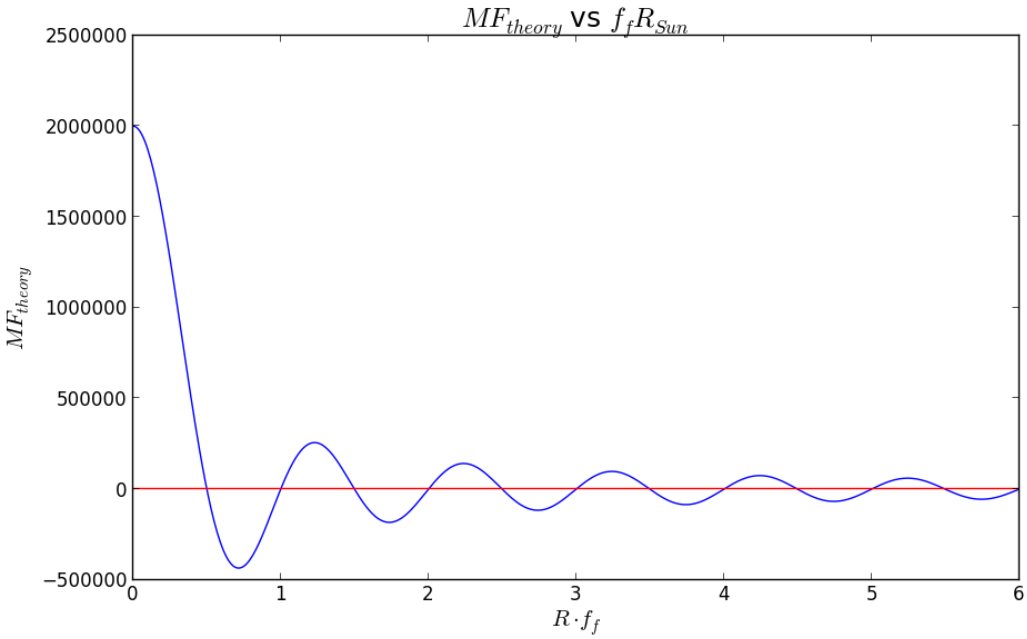

Figure 12: Theoretical Modulating Function for the Moon as a function of R_{Sun} and $f_{f,Sun}$ There are many values of $f_{f,Sun}$ at which $MF_{theory} = 0$. We chose $f_s = 115.78667$, corresponding to a radius of $R_{Sun} \approx .00432$ radian. The Sun's radius takes up .0042 radian of the 1-D sky.

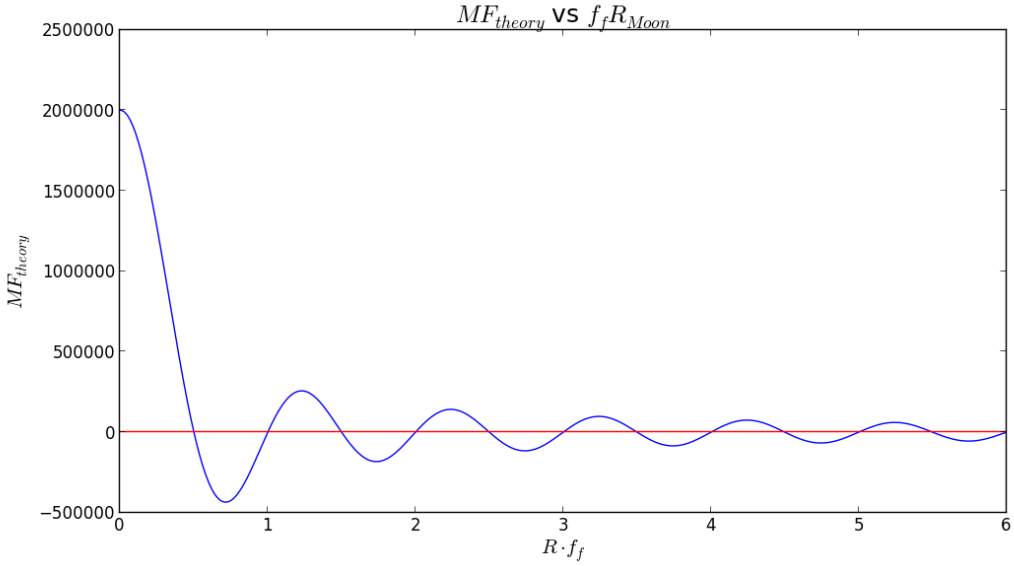

Figure 13: Theoretical Modulating Function for the Moon as a function of R_{Moon} and $f_{f,Moon}$ Similarly, we chose 356.3204 for $f_{f,Moon}$. The corresponding radius is $R_{Moon} \approx .0042$. Interestingly, the Sun and the Moon takes up the same amount of angles in the sky. By sheer coincidence, their proportional size to distance to Earth ratio, which is primarily responsible for the results of this analysis, causes near-perfect solar eclipses, a rare occurence elsewhere in the solar system.

7 Conclusion

The signal from celestial sources tell us much about their characteristics. Using interferometry, we construct fringe patterns based on phase differences among the received signals. We ultimately can derive results such as a reconstructed image of the source in the sky and characteristics such as the radius and declination of the source. Interferometry allows us to gather and analyze information sent by celestial objects to derive their intrisic qualities and even information such as the precise separation of interferometer array elements.